2024 IEEE/RSJ International Conference on Intelligent Robots and Systems (IROS)
October 14-18, 2024. Abu Dhabi, UAE

Patterned Structure Muscle : Arbitrary Shaped Wire-driven Artificial Muscle Utilizing Anisotropic Flexible Structure for Musculoskeletal Robots

Shunnosuke Yoshimura[1], Akihiro Miki[1], Kazuhiro Miyama[1], Yuta Sahara[1], Kento Kawaharazuka[1], Kei Okada[1], and Masayuki Inaba[1]

***Abstract*— Muscles of the human body are composed of tiny actuators made up of myosin and actin filaments. They can exert force in various shapes such as curved or flat, under contact forces and deformations from the environment. On the other hand, muscles in musculoskeletal robots so far have faced challenges in generating force in such shapes and environments. To address this issue, we propose Patterned Structure Muscle (PSM), artificial muscles for musculoskeletal robots. PSM utilizes patterned structures with anisotropic characteristics, wire-driven mechanisms, and is made of flexible material Thermoplastic Polyurethane (TPU) using FDM 3D printing. This method enables the creation of various shapes of muscles, such as simple 1 degree-of-freedom (DOF) muscles, Multi-DOF wide area muscles, joint-covering muscles, and branched muscles. We created an upper arm structure using these muscles to demonstrate wide range of motion, lifting heavy objects, and movements through environmental contact. These experiments show that the proposed PSM is capable of operating in various shapes and environments, and is suitable for the muscles of musculoskeletal robots.**

I. Introduction

Human muscles generate contraction movements through the exertion of force by myosin and actin filaments. Each of the tiny actuators generates contraction force, and the entire muscle contracts while maintaining the relative position of the actuators. This mechanism allows muscles to operate in various shapes, from thin muscles to wide area muscles and muscles distributed in curved shapes. Moreover, muscles can operate under contact forces from environment and deformations from other muscles' movements flexibly. Imitating this mechanism of moving the body through muscles and implementing musculoskeletal robots is important, for the purpose of creating robots closer to humans and for deepening our understanding of human structure and movement. Indeed, in the history of musculoskeletal robots, muscle actuators have been implemented using methods such as wire-driven systems and pneumatic systems [1]–[7]. However, these methods have not been able to realize the various shapes of human muscles, and operation under contact between muscles and the environment. On the other hand, in recent years, advancements in soft robotics technology and 3D printing have progressed, enabling the application of flexible mechanisms to various fields. Therefore, we propose artificial muscles for a musculoskeletal robot, called Patterned Structure Muscle (PSM), by combining wire-driven methods with soft robotics and 3D printing technologies. The overview of this research is shown in Fig. 1. In this method, the mechanism of the contraction movement of the human muscle is imitated by combining a flexible and deformable 3D pattern structure and a wire-driven mechanism. This structure has anisotropic characteristics and a wide range of motion, which allows it to operate under contact forces and flexible deformations. We create various shapes of muscles using this method, such as simple 1 degree-of-freedom (DOF) muscles, multi-DOF wide area muscles, joint-covering muscles, and branched muscles. To demonstrate the practicality of PSM and its suitability for musculoskeletal robots, we conduct three experiments. Firstly, we create muscles with various parameters, and measure their characteristics. Secondly, we confirm that the muscles of various shapes can operate individually in two different situations. Finally, we create an upper arm structure using these muscles and demonstrate its wide range of motion, lifting heavy objects, and movements through contact between the muscles and the environment.

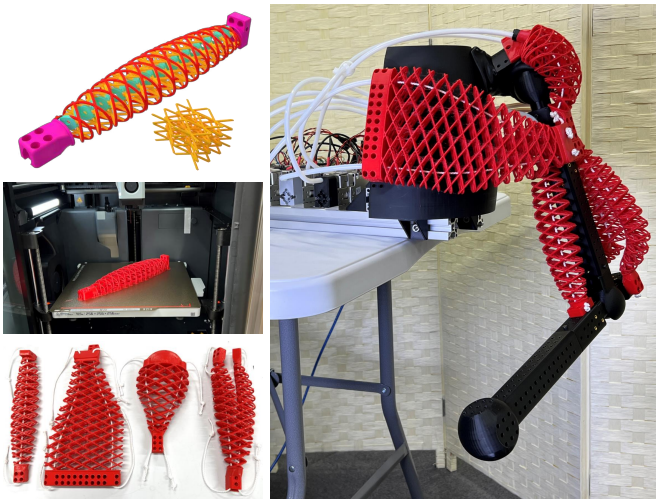

Fig. 1. The overview of this study: On the left, the structure of PSM, the process of making PSM using 3D printing, and the four types of PSM are shown. On the right, the upper arm structure driven by PSM is shown.

A. Related Work

In recent years, musculoskeletal robots have been developed, which mimic the human musculoskeletal structure. Kengoro [1] and Musashi [2] have more than 70 muscles

[1] The authors are with the Department of Mechano-Informatics, Graduate School of Information Science and Technology, The University of Tokyo, 7-3-1 Hongo, Bunkyo-ku, Tokyo, 113-8656, Japan. [yoshimura, suzuki, bando, yuzaki, kawaharazuka, okada, inaba]@jsk.t.u-tokyo.ac.jp

driven by wires, and can perform human-like movements by combining a skeletal structure and muscles. ECCE1 [3] has a wire-driven upper body structure, and Roboy [4] combines wire-driven and biological tendons. The lower-limb robot [5] developed by Kurumaya et al. uses multifilament McKibben muscles to perform simple leg movements. Ikemoto et al. have developed a shoulder complex using pneumatic actuators [6]. The Athlete Robot [7] also uses pneumatic actuators to perform dynamic movements. Thus, the actuators of musculoskeletal robots have been mainly wire-driven muscles [1]–[4] and pneumatic artificial muscles [5]–[7]. Wire-driven muscles have the advantage of being able to control the length and tension of the wire accurately, and are not dependent on the length and force of the wire so that they can be used for long contraction distances. However, they have the disadvantage of being difficult to perform contact operations with the environment, and are difficult to operate in wide and curved shapes. Pneumatic artificial muscles have the advantage of being able to exert large forces even under environmental contact, but have the disadvantage of having a limited range of motion, and there are constraints on the possible shapes of muscles that can be created.

On the other hand, the development of soft actuators using flexible materials has been advanced, which partially overcomes these weaknesses. Elastomeric Origami [8], Origami structures of various shapes [9], and 3D printed soft actuators [10], have been developed using elastomer materials with high stretchability and large deformability, but have the disadvantage of being difficult to perform contact operations and to be used for large muscles. HASEL actuator [11] and Peano-HASEL actuators [12] are electrohydraulic actuators using flexible materials, and have been applied to circular muscles [13], but it is difficult to use them for large three-dimensional muscles. Hybrid carbon nanotube yarn muscles [14] and artificial muscles from fishing line and sewing thread [15] are muscles made of threads, and have the advantage of being durable, but they do not have thickness, and are difficult to use for thick three-dimensional muscles. Fluid-driven origami-inspired artificial muscles [16] have compressible pattern structures and skins, and is able to exert large forces, but is difficult to perform contact operations due to the thin skin. Shape memory McKibben muscles [17] and high backdrivable McKibben muscles [18] have been developed, but have constraints on the adaptable muscle shape.

Thus far, with soft actuators, various methods have been proposed to achieve flexibility, high deformability, and substantial force through different materials and mechanisms. However, when it comes to practical use in combination with the skeleton of a musculoskeletal robot, challenges remain regarding applications to muscles of various shapes and environmental contact movements.

Therefore, we aim to create muscles with the following features:

- The proposed artificial muscle, PSM, combines soft robotics and wire-driven mechanisms, allowing for flexibility while enabling large force generation and long-distance contraction.
- Similar to human muscles, PSM can be created in various shapes.
- PSM can operate under environmental contact and also safely, and can be used as muscles for musculoskeletal robots by combining multiple PSMs.

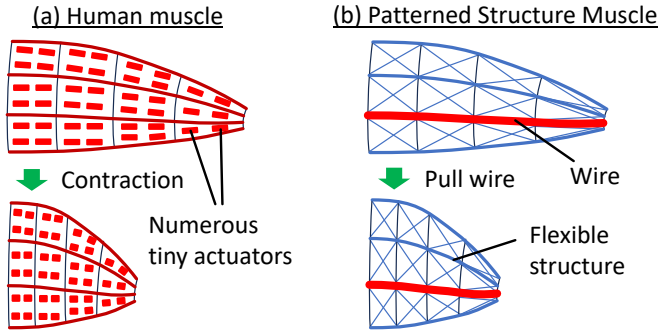

Fig. 2. Comparison between human muscle structure and the concept of PSM. While human muscle maintain their shape through the integration of small actuators during movement, PSM realizes similar movements through the combination of wire and flexible pattern structure.

II. Method

A. Concept of PSM

Human muscle structure and the concept of PSM are compared in Fig. 2. In human muscles, the myosin and actin filaments generate contraction movements, causing myofibrils and muscle fibers to exert contraction force. This mechanism, where small actuators drive while maintaining their relative positions in the muscle, enables contraction even in situations such as deformation due to external forces. In this study, we imitate this mechanism of the muscle, and realize it as a wire-driven mechanism. In traditional wire-driven muscles, a wire is stretched between the end points of the muscle, and contraction is induced by winding the wire with a motor. However, because the wire itself lacks thickness, structures resembling various shapes of human muscles such as sheet-like muscles cannot be achieved as they are. Additionally, since the wire is stretched linearly, performing actions with curved shapes is also challenging. Therefore, we aim to address these issues through the following approach. The wire is routed along the path of a single muscle fiber between the endpoints of the muscle. In areas without wire, flexible structure is created to deform while maintaining the shape of the muscle in accordance with the contraction of the wire. This allows for movements that are closer to human muscles. To realize this structure, the requirements of the muscle structure can be described as the following three directions of characteristics, as shown in Fig. 3.

- x-direction: Flexibility and range of motion to realize self-contraction and extension from external tension.
- y-direction: Strength that supports the muscle structure and allows contraction in the x-direction even in the presence of external load in the y-direction.

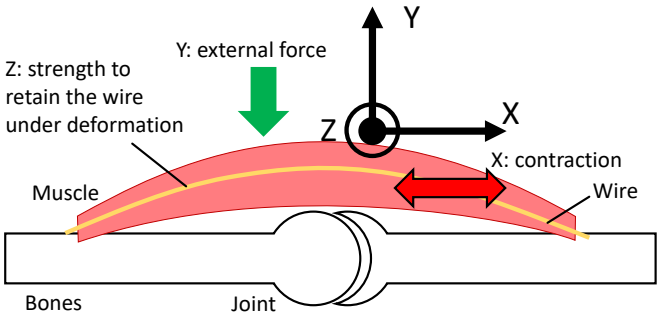

Fig. 3. The three directions of characteristics required for PSM. In x-direction, flexibility and range of motion are required to realize contraction. In y-direction, strength is required to support the structure and allow x-directional contraction in the presence of external load. In z-direction, a certain degree of strength is required to maintain the positional relationship of wire and structure.

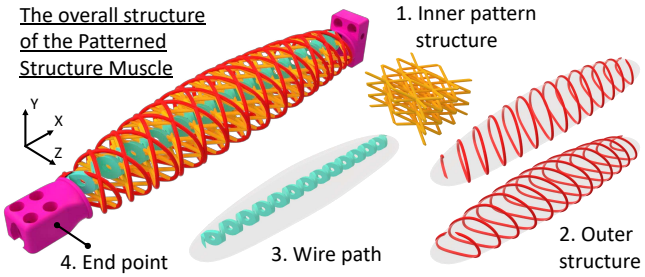

Fig. 4. PSM is composed of the following four structures: 1. inner pattern structure, 2. outer structure, 3. wire path, and 4. end points.

- z-direction: A certain degree of strength to maintain the positional relationship of wire and surrounding structure in the muscle, while preserving the route of wire.

B. Mechanism of PSM

PSM is composed of the following four structures, shown in Fig. 4: 1. inner pattern structure, 2. outer structure, 3. wire path, and 4. end points. The end points are attached to the bone. Wire is passed through the wire path and the end points. When the wire is pulled, the inner pattern structure, wire path, and outer structure are compressed between the end points, resulting in contraction of the entire muscle. The inner pattern structure, as shown in Fig. 5, is a critical part that has the most significant impact on the properties of PSM. The inner structure of PSM is formed by arranging pattern unit structures periodically in the x, y, and z directions. This pattern unit structure is composed of multiple branches. The structure is called lattice structure, and various representative shapes exist [19]. The lattice structure is well suited to additive manufacturing [20], and is expected to be widely used, from metal components [21] to damping mechanism [22]. In the lattice structure we use, the length of the unit pattern in the x, y, and z directions are denoted as x, y, z, as shown in Fig. 5 (a). The diameter of the branches is denoted as p. These x,y,z directions correspond to the directions mentioned in Fig. 3. The characteristics of the compression deformation are considered in two deformation phases:

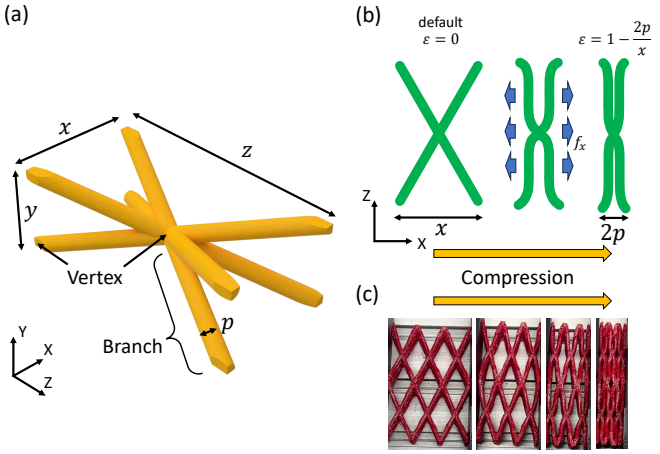

Fig. 5. The inner pattern structure of PSM utilize the lattice structure. (a) illustrates the unit structure, (b) illustrates the deformation during compression, and (c) shows actual images of the deformation.

1) Bending deformation phase: Let's consider three compressions along the x, y, and z directions, respectively. Let the nominal strain of each compression be ε. Until the branches come into contact, deformation occurs within the range of $0 \leq \varepsilon \leq 1-2p/x$, $0 \leq \varepsilon \leq 1-2p/y$, $0 \leq \varepsilon \leq 1-2p/z$, leading to a reduction in the angle and distance between the branches, as shown in Fig. 5 (b). In this state, the overall compression occurs due to a large bending of the branches near the vertices, and a small bending near the center of the branches. The actual compression process is shown in Fig. 5 (c). We call this state the bending deformation phase. In this deformation, the magnitude relationship between x, y, and z align with the deformation magnitudes of the branches in their respective compression directions. Consequently, the magnitude relationship for x, y, and z, as well as the repulsive forces per unit pattern for each direction, f_x, f_y, and f_z, are consistent. Also, the larger the p, the larger the deformation volume, and the larger these forces. The average nominal stress in compression is expressed as follows:

$$\sigma_x = \frac{f_x}{yz}, \sigma_y = \frac{f_y}{xz}, \sigma_z = \frac{f_z}{xy} \tag{1}$$

From these expressions, we obtain the following properties:

- The order of magnitudes of x, y, and z corresponds to the order of magnitudes of σ_x, σ_y, and σ_z.
- Increasing the diameter p results in larger values for σ_x, σ_y, and σ_z.
- Enlarging x, y, and z individually leads to larger bending deformation regions in the corresponding x, y, and z directions.

2) Compression deformation phase: When $\varepsilon > 1-2p/x$, $\varepsilon > 1-2p/y$, and $\varepsilon > 1-2p/z$ in corresponding compression directions, the branches come into contact, and overall compressive deformation of the material occurs. We call this state the compression deformation phase. In general, the pressure during compression deformation phase is larger than the pressure during bending deformation phase.

In the design of PSM, the two phases of deformation

are utilized. By setting the parameters such that $y \leq x \leq z$, the following properties can be obtained: First, by reducing the value of y in comparison to x and z, the structure can transition to the compression deformation phase with a small amount of deformation. At the beginning of the deformation, the structure is soft, but after a small deformation, the structure becomes stiff and can support a large load. Second, by setting the value of x to be the second largest, the contraction distance of x direction in the bending deformation phase is made larger than that in the y direction, and the repulsive force of x direction, f_x, during the bending deformation phase is not as large as that in the z direction. This means that the structure is flexible in the x-direction, enabling substantial contraction over long distances. Finally, by setting the value of z to be the largest, the pressure during bending deformation in the z direction is made the largest. This ensures a certain degree of structural support strength to maintain the wire path and overall shape. These properties satisfy the requirements of x, y, and z directions mentioned in II-A. While utilizing the characteristics of the inner pattern structure described above, the wire path, outer pattern as a muscle surface and endpoints for connection with the bone are realized. The wire path and outer pattern are arranged by taking the y-directional projection of the inner pattern based on the shapes of the tubes for threading wires and the muscle surface, as illustrated in Fig. 4 (3, 2). This allows these parts to function without interfering with the x-directional deformation, y-directional load support, and z-directional internal structural support. Also, the end points (Fig. 4 (4)) are composed of simple dense structure that is suitable for attachment. In summary, PSM utilizes the three directions of anisotropic characteristics, and the combination of sparse lattice structure and dense parts, to achieve various properties with a single material.

C. Process of Making PSM

The process of making PSM is shown in Fig. 6. This process consists of modeling, 3D printing, and attaching wires and motors. In the modeling process, the overall shape of the muscle and the route of the wire are determined firstly, and then they are converted into a pattern structure. We generate pattern structure from the shape, route and structural parameters x, y, z, p by a script. Then, PSM is created by FDM 3D printing using Thermoplastic Polyurethane (TPU) as the material. Finally, wires and motors are attached to complete the assembly.

Using FDM 3D printing, it is possible to create various shapes. Also, it is relatively inexpensive, readily available, and easy to use, and does not require special skills or post-processing.

D. Various Shapes of PSM and Upper Arm Using PSM

Utilizing the basic characteristics of PSM described so far, we created four types of PSM. As shown in Fig. 7, these are, muscle 1: simple single muscle, muscle 2: wide sheet-like muscle, muscle 3: muscle that covers a joint, and muscle 4: branched muscle. Except for the simple single

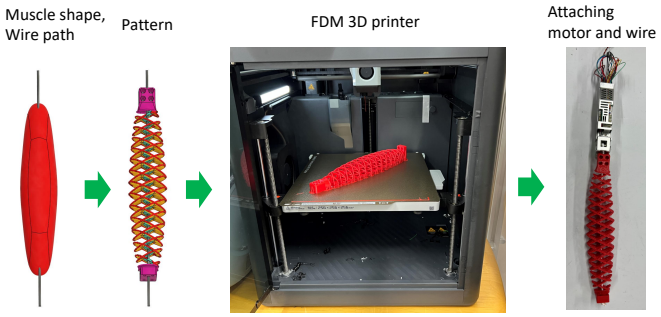

Fig. 6. The making process of PSM consists of four steps: 1. modeling muscle shapes and wire path, 2. converting them into pattern structure, 3. FDM 3D printing, and 4. attaching wires and motors.

TABLE I
SPECIFICATIONS OF MUSCLE 1

Parameter	Value
Pattern size parameter (x,y,z)	(15, 10, 30) [mm]
Pattern branch diameter	2 mm
Muscle size (X,Y,Z)	(250, 30, 50) [mm]
Length after contraction in the x-axis	115 mm
Length after stretching in the x-axis	380 mm
Range of twisting in the x-axis	over ±360 deg
Bending in the y and z axes	over ±360 deg
Mass of PSM	38 g
Material of PSM	TPU 95A
Maximum tension of the motor-wire unit	300 [N]
Maximum speed of the motor-wire unit	250 [mm/s]

muscle, all of them are 2-DOF muscles. The muscle that covers a joint has a round shape to cover the interior, and the branched muscle is created to have two branches that contract separately. The pattern parameters were standardized to (x, y, z, p) = (15, 10, 30, 2) (mm). Specifically, the specifications of a simple single muscle is presented in Table I. These muscles flexibly deform in response to external forces. In particular, photographs illustrating the deformation of PSMs by hand are presented in Figure 8. While flexibly deforming in response to external forces, they also protect the wire and its path.

Furthermore, we created an upper arm structure, as shown in Fig. 9, by combining these muscles. It consists of bones and joints printed with PLA, and PSMs made from TPU. The motor-wire units from previous research [2] are used, and the wires are passed from the motors to the muscles through PTFE tubes. The joint structure includes a 3-DOF ball joint at the shoulder, and a 2-DOF joint at the elbow that enables flexion, extension, as well as internal and external rotation. The muscle 1,2,3,4 described above are placed at the positions of the biceps brachii, pectoralis major, deltoid, and triceps brachii. In addition, a single muscle (muscle 5) is added as the back muscle. This structure was created to demonstrate the potential of PSM, and is not intended to strictly mimic the human musculoskeletal structure.

III. EXPERIMENTS

A. Measurement of PSM Properties With Varied Parameters

First, we measure the anisotropic characteristics of PSM. We created six inner structures and PSMs with different

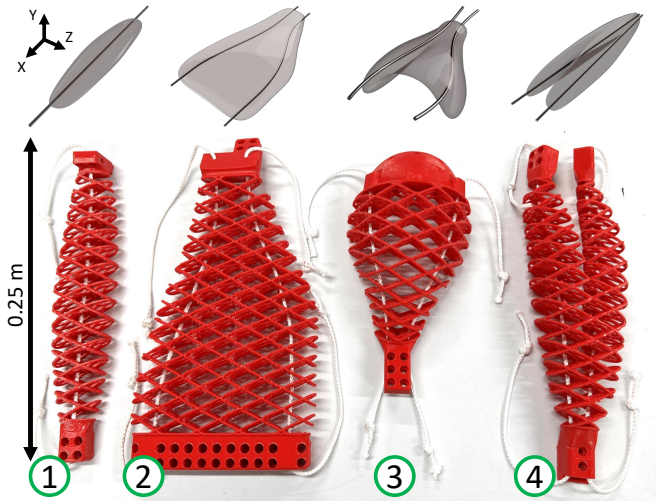

Fig. 7. The four shapes of PSM: Muscle 1 is a simple single-wire muscle, muscle 2 is a wide sheet-like muscle. muscle 3 is a muscle covering a joint, and muscle 4 is a branched muscle. muscle 2,3,4 are 2-DOF muscles.

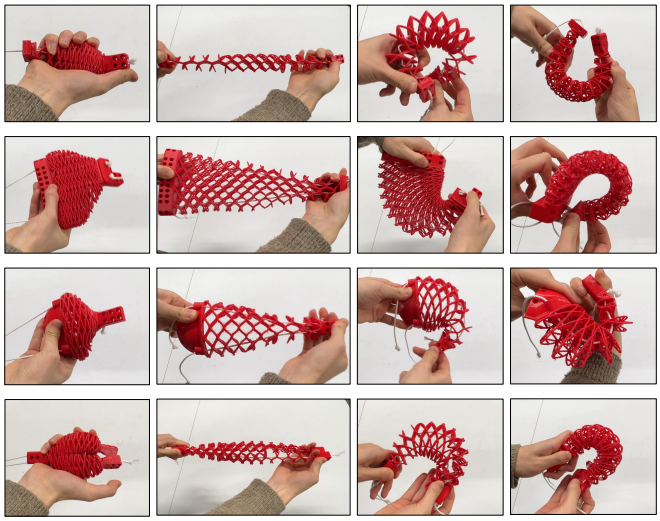

Fig. 8. The deformation of muscles 1, 2, 3, and 4 are illustrated from top to bottom. In the leftmost column, the deformation caused by pulling the wire are shown. On the right side, the stretching deformation in the x-axis, and the bending deformation in the y and z axes are shown.

pattern parameters (x, y, z, p), to measure their compression characteristics. Condition A has the reference parameters (15, 10, 30, 2) (mm), and B, C have thickness p as 1.5 and 2.5, respectively. D, E, F have altered x, y, z to 20, 5, 20 from A's parameters, respectively. For measurements, inner structures with pattern numbers of 3, 3, 2 for x, y, z were used. The characteristics of PSM were measured using muscles with dimensions of approximately 75 x 30 x 45 (mm). In the case of D, E, F, the size of the entire muscle shapes was multiplied by the ratio of the pattern length, and the pattern numbers and arrangement were the same as A.

In Fig. 10, the nominal pressure-strain curves of the internal structure are shown. The color of each line in the graph corresponds to the color of the x,y,z in the graph

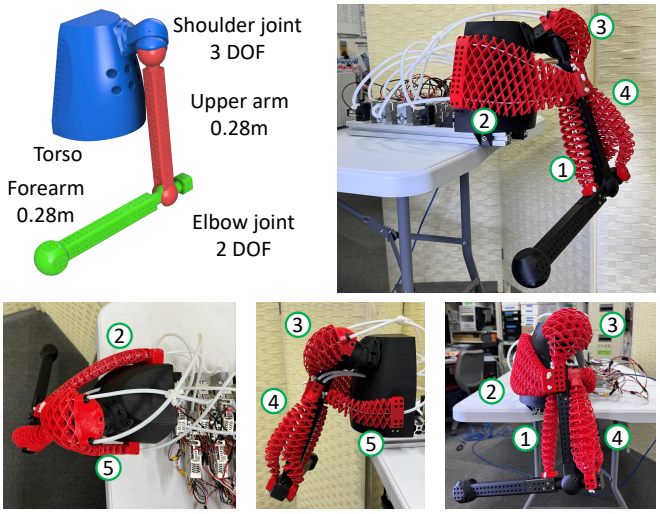

Fig. 9. The upper arm structure combining PSMs. Muscle 1 is positioned for the biceps brachii, muscle 2 for the pectoralis major, muscle 3 for the deltoid, and muscle 4 for the triceps brachii. An additional muscle (muscle 5) is added as the back muscle. Note that this design was created to demonstrate the feasibility of using PSM as muscles, and is not intended to strictly mimic the human musculoskeletal structure.

title. First, especially for the x and y directions, it can be observed that the pressure increases rapidly when the strain reaches around 0.6, indicating a transition from the bending deformation phase to the compression deformation phase. Generally, the pressure during bending deformation is large depending on the size of x, y, and z. It means that adjusting these size relationships makes it possible to control the anisotropic characteristics.

In Fig. 11, the force-displacement curves of PSMs are shown. In the x and z directions, bending deformation occurs over a wide area. The x-direction is soft and suitable for contraction, while the z-direction is relatively rigid and suitable for maintaining shape. In the y-direction, there is a transition to compression deformation phase with slight deformation, making it the strongest. This is due to not only the size of y, but also the presence of internal wire paths, which reduce the bending deformation region of the y-direction. In summary, it is shown that PSM has anisotropic characteristics utilizing the pattern structure, and also that these characteristics can be adjusted by changing the pattern parameters.

B. Contraction Motion of PSM

Next, the performance of the four types of PSM created (Fig. 7) are tested in two different environments. To confirm its ability to exert large contraction force, a total weight of 10 kg was lifted using the PSM, as shown in Fig. 12. Also, to demonstrate its movements under contact, weights of 1.25 kg or 1.38 kg were placed or leaned on the horizontally positioned PSM, and the contraction was performed, as shown in Fig. 13. At the top of the each figure, the PSMs' contraction are shown. The muscle number and time are shown as 1-a, 1-b, etc. At the bottom, the current and wire length of each muscle are shown. In muscles with

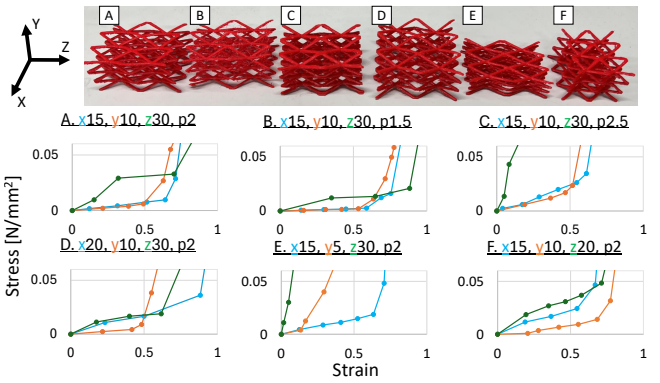

Fig. 10. Compression measurements on internal structures. Displaying nominal stress-strain curves for six inner structures with different pattern parameters.

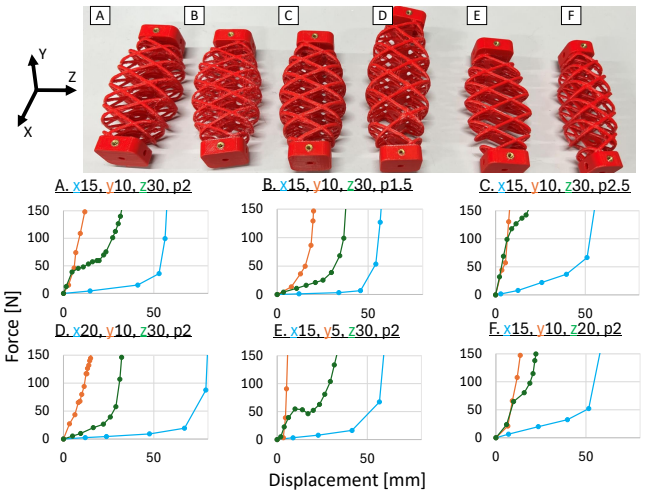

Fig. 11. Compression measurements on PSMs. Displaying force-displacement curves for six muscles with different pattern parameters.

multiple degrees of freedom, such as Muscle 2, 3, 4, the contraction is performed by contracting one side first, and then both sides, and finally the opposite side. The plots for the 2-DOF muscles are overlaid in the graph. In the initial experimental setup, it was confirmed that the PSM is capable of lifting heavy objects. Furthermore, in the second experimental environment, it was verified that the PSM can operate under the load from the environment. In muscles 2, 3, and 4, 2-DOF movements such as contraction on only one side, contraction on both sides simultaneously, were performed, utilizing the interaction of the two wires. In these cases, the structure around the wire paths and the wire paths themselves undergo deformation while maintaining their internal positional relationships, as described in Fig. 2. These results show that PSM can utilize the advantages of wire-driven actuation, such as the ability to exert large forces and control the length of the wire accurately, depending on the motor. Additionally, it demonstrates that even in the presence of environmental contact, the deformation of wire paths remain stable, overcoming the weaknesses of wire-driven actuation.

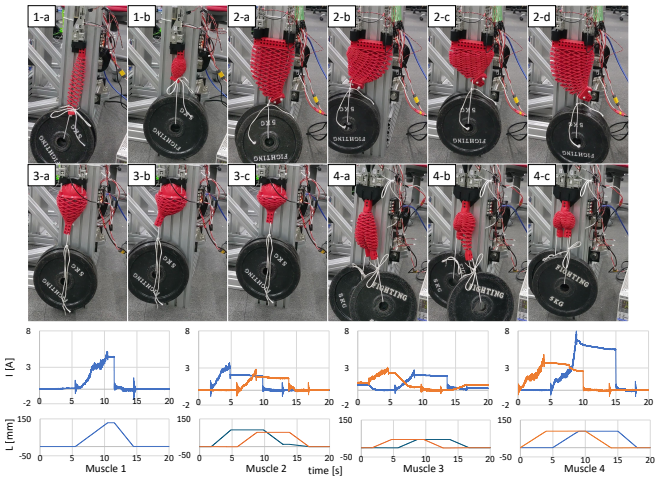

Fig. 12. With each shape of PSM shown in Fig. 7, a total of 10kg weight was lifted. In the 2-DOF muscles, two wires were operated independently.

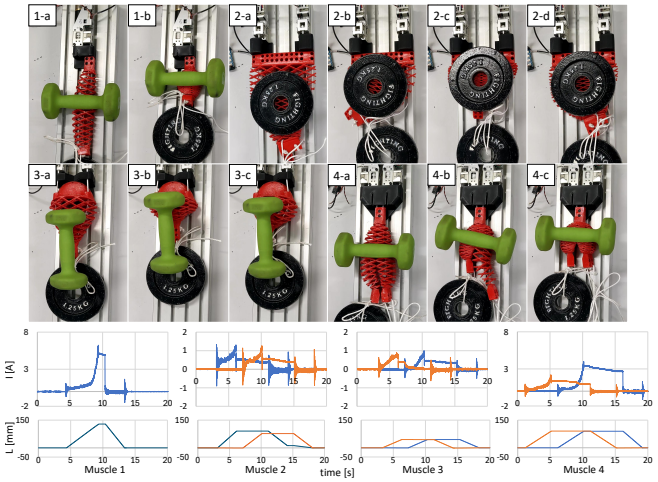

Fig. 13. We performed the same contraction motion as in Fig. 12, with the muscle placed horizontally and the weight leaning against it, confirming its operation under contact. The green weight is 1.38kg, and the black weight is 1.25kg. Each of the PSMs pulls one or two 1.25kg weights.

C. Motion of The Arm Constructed with PSM

In this experiment, we demonstrate the operation of the upper arm structure shown in Fig. 9. Firstly, we perform the motion of lifting a weight using the muscle 1, located at the position of the biceps brachii, as shown in Fig. 14. We send position commands to the motor and make the elbow flex with a 1.38kg weight attached to the hand. The flexion is carried out over 7 seconds, making the forearm almost horizontal. The arm keeps the position for 5 seconds, and then extends over 5 seconds. When calculated from the moment arm of the muscle 1, a load of about 200N is applied to the muscle. This is within the capacity of the motor unit used, and the lifting is successful. As shown in III-B, the tensile load of PSM is supported by the motor and wire. Therefore, PSM can exert a large tensile force according to the performance of the motor. This capability is also effective in applications for robots, such as the motion of lifting a weight in the upper arm.

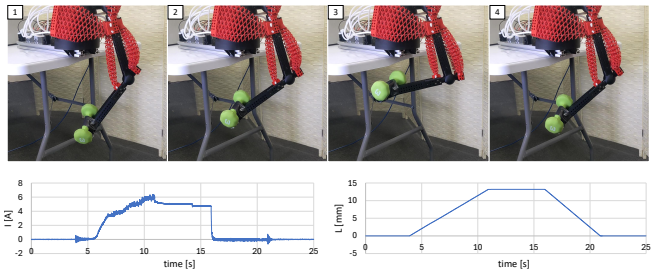

Fig. 14. We conducted a motion experiment lifting a 1.38kg weight attached to the hand using muscle 1 at the position of the biceps brachii in the upper arm. We only plot the current and length of muscle 1 in this experimental setup, because other muscles' current and length are almost constant.

Next, we perform a motion of the entire upper arm for about 30 seconds, as shown in Fig. 15. The top of the figure shows the motion, and the bottom shows the current and wire length of each muscle. The plots for Muscle 1 and Muscle 5 as described in Fig. 9 were overlaid. The format of the plots for the other muscles is the same as that in Fig. 12. This motion consists of 8 postures: 1. arm down, 2. elbow flexion, 3. forearm pronation, 4. forearm supination, 5. raise upper arm, move hand forward, 6. raise upper arm further, pull hand backward, 7. lower upper arm backward, 8. bring hand to the front of the chest. Firstly, the pronation and supination of the forearm are performed using the branched muscle, which is placed at the position of the triceps brachii. It achieves a rotation of ± 30 degrees. Secondly, in the motion of raising the upper arm, the two degrees of freedom of the deltoid are utilized to move the upper arm forward, middle, and backward. While the muscle has a round shape that covers the joint, it can function as a muscle. After that, the motion of bringing the hand to the front of the chest is performed using muscle 2, the pectoralis major. The motion is performed with a small current due to the presence of two wires. Due to the interaction among muscles, each muscle undergoes deformation in bending or stretching in response to the contraction of other muscles. Even in such situations, PSMs maintain their own structure and deform and operate while preserving the wire path. This contributes to the wide range of motion of the hand from the back to the front. Through this experiment, it has been demonstrated that PSM can be used as muscle in an actual musculoskeletal robot. Its capability to be created in various shapes and multi-DOF makes it useful in the construction of musculoskeletal robots.

Furthermore, we performed simplified movements, such as raising the upper arm and bringing the hands in front of the chest, in situations involving environmental contacts. This is illustrated in Fig. 16. Under the first two conditions, the upper arm was moved with two types of bags put on the shoulder, containing 1.38kg weights. The bags were placed to make contact with the pattern parts of the deltoid, the pectoralis major mainly. In particular, 75% of the contact area of the bag on the shoulder was directly in contact with the pattern part of the deltoid, and the remaining 25% was in contact with the end point of the deltoid. In such situations

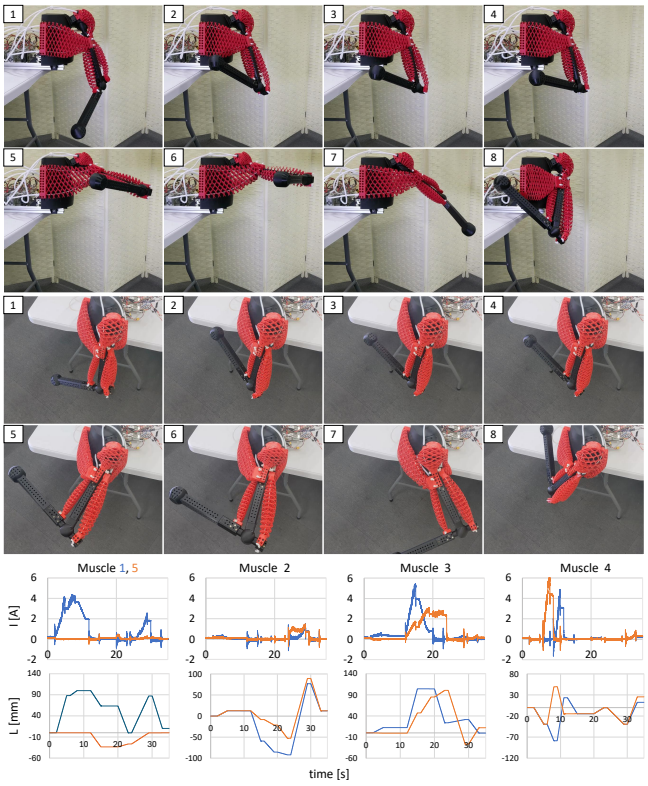

Fig. 15. A series of movements are performed using the upper arm structure. It consists of 8 postures, and the motion is performed for about 30 seconds. The arm utilizes muscles such as covering joints and branched muscles, and the wide range of motion is achieved. The muscles interact with each other, undergoing bending and tensile deformation by the contraction of other muscles, yet they still function as muscles under these conditions.

where the muscles are loaded by environmental contacts, PSM is able to operate, allowing the upper arm to move. Also, in the remaining two conditions, the upper arm was moved with cloth wrapped around the structure, and with a person directly touching the pattern part of the deltoid. From the third experimental condition, it was confirmed that the motion could be performed without catching the cloth at their muscles and joints. From the final experimental condition, it was shown that safety is ensured by covering joints and wires with muscles composed of flexible materials, and even when the muscles are touched directly by a person, the operation can be performed. In summary, using PSM as muscle in a musculoskeletal robot allows for safe movements in various environments, involving environmental contacts.

IV. Conclusion

In this study, we proposed Patterned Structure Muscle (PSM), which can be used as a muscle for musculoskeletal robots. In the design of PSM, we utilized the anisotropic characteristics of the pattern structure, FDM 3D printing of flexible material TPU, and wire-driven actuation. This approach allows for the movement of muscles with various shapes and degrees of freedom under environmental contact forces. In the experiment, we confirmed the lifting of heavy objects and operation under environmental contact in various

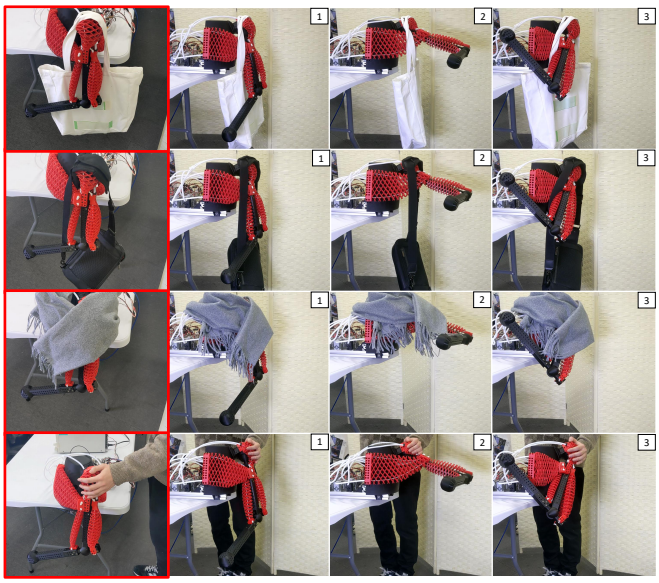

Fig. 16. Upper arm motion in situations where muscles come into direct contact with the environment. Even in scenarios involving contact with bags, fabric, or hands, the muscles operate safely while withstanding external contact loads.

shapes of PSMs. We also confirmed that in the upper arm structure composed of multiple PSMs, strong movements, a wide range of motion, and environmental contact operations are achieved. All of these results demonstrate that PSM is suitable for use as muscles in musculoskeletal robots.

PSM is highly scalable because of its sparse-structure and 3D printing making process. By using conductive filaments to detect deformation or embedding sensors, it is believed that various functionalities, including tactile sensing, will be achieved. Also, in the future, we will create a musculoskeletal humanoid with a structure that mimics the human body using PSM. We think that PSM will enable body movements closer to those of human, because PSM can imitate the complex shapes, roles and movements of vairous human muscles. Furthermore, by utilizing environmental contact performance and safety, it is believed that significant interactions with external environments and humans, such as rolling over motiom or hugging, will be realized.

REFERENCES

[1] Y. Asano, T. Kozuki, S. Ookubo, M. Kawamura, S. Nakashima, T. Katayama, Y. Iori, H. Toshinori, K. Kawaharazuka, S. Makino, Y. Kakiuchi, K. Okada, and M. Inaba, "Human Mimetic Musculoskeletal Humanoid Kengoro toward Real World Physically Interactive Actions," in *Proceedings of the 2016 IEEE-RAS International Conference on Humanoid Robots*, 2016, pp. 876–883.

[2] K. Kawaharazuka, S. Makino, K. Tsuzuki, M. Onitsuka, Y. Nagamatsu, K. Shinjo, T. Makabe, Y. Asano, K. Okada, K. Kawasaki, and M. Inaba, "Component modularized design of musculoskeletal humanoid platform musashi to investigate learning control systems," in *2019 IEEE/RSJ International Conference on Intelligent Robots and Systems (IROS)*, 2019, pp. 7300–7307.

[3] H. G. Marques, M. Jäntsch, S. Wittmeier, O. Holland, C. Alessandro, A. Diamond, M. Lungarella, and R. Knight, "Ecce1: The first of a series of anthropomimetic musculoskeletal upper torsos," in *2010 10th IEEE-RAS International Conference on Humanoid Robots*. IEEE, 2010, pp. 391–396.

[4] P.-A. Mouthuy, S. Snelling, R. Hostettler, A. Kharchenko, S. Salmon, A. Wainman, J. Mimpen, C. Paul, and A. Carr, "Humanoid robots to mechanically stress human cells grown in soft bioreactors," *Communications Engineering*, vol. 1, no. 1, p. 2, 2022.

[5] S. Kurumaya, K. Suzumori, H. Nabae, and S. Wakimoto, "Musculoskeletal lower-limb robot driven by multifilament muscles," *Robomech Journal*, vol. 3, pp. 1–15, 2016.

[6] S. Ikemoto, F. Kannou, and K. Hosoda, "Humanlike shoulder complex for musculoskeletal robot arms," in *2012 IEEE/RSJ International Conference on Intelligent Robots and Systems*, 2012, pp. 4892–4897.

[7] R. Niiyama, S. Nishikawa, and Y. Kuniyoshi, "Athlete robot with applied human muscle activation patterns for bipedal running," in *Proc. IEEE-RAS Int. Conf. on Humanoid Robots (Humanoids 2010)*, Nashville, Tennessee USA, Dec. 2010, pp. 498–503.

[8] R. V. Martinez, C. R. Fish, X. Chen, and G. M. Whitesides, "Elastomeric origami: Programmable paper-elastomer composites as pneumatic actuators," *Advanced Functional Materials*, vol. 22, no. 7, pp. 1376–1384, 2012.

[9] Z. Jiao, C. Zhang, W. Wang, M. Pan, H. Yang, and J. Zou, "Advanced artificial muscle for flexible material-based reconfigurable soft robots," *Advanced Science*, vol. 6, no. 21, p. 1901371, 2019.

[10] M. Schaffner, J. A. Faber, L. Pianegonda, P. A. Rühs, F. Coulter, and A. R. Studart, "3d printing of robotic soft actuators with programmable bioinspired architectures," *Nature communications*, vol. 9, no. 1, p. 878, 2018.

[11] E. Acome, S. K. Mitchell, T. G. Morrissey, M. B. Emmett, C. Benjamin, M. King, M. Radakovitz, and C. Keplinger, "Hydraulically amplified self-healing electrostatic actuators with muscle-like performance," *Science*, vol. 359, no. 6371, pp. 61–65, 2018.

[12] N. Kellaris, V. G. Venkata, G. M. Smith, S. K. Mitchell, and C. Keplinger, "Peano-hasel actuators: Muscle-mimetic, electrohydraulic transducers that linearly contract on activation," *Science Robotics*, vol. 3, no. 14, p. eaar3276, 2018.

[13] X. Wang, S. K. Mitchell, E. H. Rumley, P. Rothemund, and C. Keplinger, "High-strain peano-hasel actuators," *Advanced Functional Materials*, vol. 30, no. 7, p. 1908821, 2020.

[14] M. D. Lima, N. Li, M. J. de Andrade, S. Fang, J. Oh, G. M. Spinks, M. E. Kozlov, C. S. Haines, D. Suh, J. Foroughi, S. J. Kim, Y. Chen, T. Ware, M. K. Shin, L. D. Machado, A. F. Fonseca, J. D. W. Madden, W. E. Voit, D. S. Galvo, and R. H. Baughman, "Electrically, chemically, and photonically powered torsional and tensile actuation of hybrid carbon nanotube yarn muscles," *Science*, vol. 338, no. 6109, pp. 928–932, 2012.

[15] C. S. Haines, M. D. Lima, N. Li, G. M. Spinks, J. Foroughi, J. D. W. Madden, S. H. Kim, S. Fang, M. J. de Andrade, F. Gktepe, zer Gktepe, S. M. Mirvakili, S. Naficy, X. Lepr, J. Oh, M. E. Kozlov, S. J. Kim, X. Xu, B. J. Swedlove, G. G. Wallace, and R. H. Baughman, "Artificial muscles from fishing line and sewing thread," *Science*, vol. 343, no. 6173, pp. 868–872, 2014.

[16] S. Li, D. M. Vogt, D. Rus, and R. J. Wood, "Fluid-driven origami-inspired artificial muscles," *Proceedings of the National Academy of Sciences*, vol. 114, no. 50, pp. 13 132–13 137, 2017.

[17] K. Takashima, J. Rossiter, and T. Mukai, "Mckibben artificial muscle using shape-memory polymer," *Sensors and Actuators A: Physical*, vol. 164, no. 1, pp. 116–124, 2010.

[18] G. Na, H. Nabae, and K. Suzumori, "Braided thin mckibben muscles for musculoskeletal robots," *Sensors and Actuators A: Physical*, vol. 357, p. 114381, 2023.

[19] A. Seharing, A. H. Azman, and S. Abdullah, "A review on integration of lightweight gradient lattice structures in additive manufacturing parts," *Advances in Mechanical Engineering*, vol. 12, no. 6, p. 1687814020916951, 2020.

[20] W. Tao and M. C. Leu, "Design of lattice structure for additive manufacturing," in *2016 International Symposium on Flexible Automation (ISFA)*, 2016, pp. 325–332.

[21] L.-Y. Chen, S.-X. Liang, Y. Liu, and L.-C. Zhang, "Additive manufacturing of metallic lattice structures: Unconstrained design, accurate fabrication, fascinated performances, and challenges," *Materials Science and Engineering: R: Reports*, vol. 146, p. 100648, 2021.

[22] E. C. Clough, T. A. Plaisted, Z. C. Eckel, K. Cante, J. M. Hundley, and T. A. Schaedler, "Elastomeric microlattice impact attenuators," *Matter*, vol. 1, no. 6, pp. 1519–1531, 2019.